Electronic structure of self-assembled InGaAs/GaAs quantum rings studied by capacitance-voltage spectroscopy

W. Lei,[1,2,a] C. Notthoff,[1] A. Lorke,[1] D. Reuter,[3] and A. D. Wieck[3]
[1]*Fachbereich Physik and CeNIDE, Universität Duisburg-Essen, Lotharstr. 1, 47048 Duisburg, Germany*
[2]*Department of Electronic Materials Engineering, RSPE, Australian National University, Acton, Canberra ACT 0200, Australia*
[3]*Fakultät für Physik, Ruhr-Universität Bochum, Universitätsstr. 150, 44780 Bochum, Germany*

(Received 23 September 2009; accepted 22 December 2009; published online 22 January 2010)

Self-assembled InGaAs quantum rings, embedded in a GaAs matrix, were investigated using magneto-capacitance-voltage spectroscopy. The magnetic-field dispersion of the charging energies exhibits characteristic features for both the first and second electron, which can be attributed to a ground state transition from $l=0$ into $l=-1$, and a ground state transition from $l=-1$ into $l=-2$, respectively. Furthermore, using a combination of capacitance-voltage spectroscopy and one-dimensional numerical simulations, the conduction band structure of these InGaAs quantum rings was determined. © *2010 American Institute of Physics*. [doi:10.1063/1.3293445]

Recent advances in the growth technology of semiconductor nanostructures make it possible to fabricate defect-free semiconductor nanostructures with various geometries.[1–3] Because of their peculiar magnetic properties, there has been particular interest in volcano-shaped semiconductor quantum rings (QRs). Like self-assembled quantum dots (QDs), QRs also demonstrate atomlike properties,[2,4] which indicates their great potential for device applications in optics, optoelectronics, quantum cryptography, and quantum computing. For improved device performance, it is essential to know the electronic properties of the QRs. Although much attention has been paid to understanding the electronic properties of QRs theoretically,[5] only very little experimental data are available on the QRs.[2,6–8] As shown by the work on QDs,[9,10] capacitance-voltage (C-V) spectroscopy can provide valuable information about the carrier charging in the sample structure, which provides an access to understanding the electronic properties of the QRs.

In this letter, we present a C-V spectroscopy study on self-assembled InGaAs/GaAs QRs, in a magnetic field B, applied perpendicularly to the plane of the rings. With increasing the magnetic field, remarkable changes in the magnetic-field dispersion of the energies of the singly and doubly charged QRs are observed around 2.8 and 5.8 T, which are attributed to a ground state transition from $l=0$ to $l=-1$ and a ground state transition from $l=-1$ to $l=-2$, respectively. These C-V data, combined with a self-consistent numerical solution of the one-dimensional (1D)-Schrödinger/Poisson equations, allow it to determine the electron energy levels of the QRs with respect to the GaAs conduction band edge.

The investigated sample was grown on semi-insulating (001) GaAs substrate in a solid-source molecular beam epitaxy system. The active part of the sample was grown using the following layer sequence: first, a 60 nm thick, heavily Si-doped GaAs back contact layer, then 25 nm of undoped GaAs as a tunneling barrier, then 1.4–1.7 ML In(Ga)As QR layer (first 1.4–1.7 ML InAs was deposited at 585 °C to form QDs, then the QDs were capped by 2 nm GaAs at 545 °C, after that a 30s growth interruption was introduced[2,11]), then 30 nm GaAs (spacer layer) and 34 periods of a AlAs (3 nm)/GaAs (1 nm) superlattice as the blocking layer, followed by a 5 nm thick GaAs cap layer. As a confirmation for the ring formation and for atomic force microscopy (AFM) imaging, the deposition of the ring layer was repeated on the surface, using identical growth conditions. To ensure that the rings maintain their shape during overgrowth,[12] the temperature was lowered before the deposition of the spacer layer. The n^+-doped GaAs back contact layer was contacted from the sample surface by an AuGe alloy, annealed at $T=450°$. Subsequently, a NiCr Schottky gate electrode (780×780 μm^2) was prepared. C-V characteristics of the sample were measured by superimposing a dc gate bias (V_g) with a small ac voltage (5 mV rms) of variable frequency (f). Standard lock-in technique was used to record the capacitance signal. Whenever the chemical potential of the back contact (Fermi energy) is in resonance with the discrete energy levels in the InGaAs QRs, resonant tunneling occurs and the capacitance signal shows characteristic peaks. Similarly, the C-V spectra exhibit steps when the InAs wetting layer (WL), or the two-dimensional electron gas (2DEG), formed at the interface between the GaAs spacer layer and the AlAs/GaAs superlattice, become occupied.[10,13,14] A schematic profile of the conduction band edge of the sample is shown in Fig. 1(a). The structure parameters l_1, l_2, and l_0 in Fig. 1(a) are the distance from the back contact to the QR layer, 2DEG, and sample surface, respectively. E_1 and E_2 in Fig. 1(a) represent the energy difference between the Fermi energy and the GaAs conduction band edge at the position of the QR layer and the 2DEG, respectively. All C-V measurements were taken at 4.2 K.

The inset of Fig. 1(b) shows an AFM image of the sample surface. The InGaAs QRs are well developed with a height of about 2 nm, an outer diameter of about 49 nm, and an inner diameter of about 20 nm. How this compares to the energetic structure of the embedded InGaAs rings will be discussed below. A typical C-V spectrum of the sample taken at $f=8113$ Hz and the second derivative of the C-V trace are shown in Fig. 1(b). Clearly, at least four charging features can be observed in Fig. 1(b), which are labeled as s_1 (0.489

[a]Electronic addresses: wen.lei@uni-due.de and wen.lei@anu.edu.au.

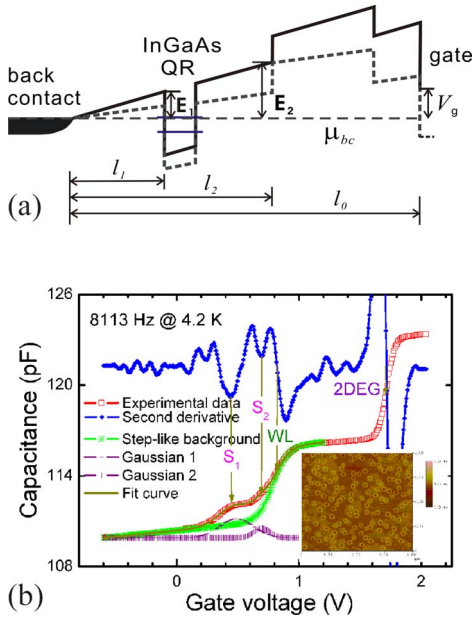

FIG. 1. (Color online) Schematic profile of the conduction band edge of the sample (a), and typical C-V spectrum of the QRs, its second derivative, and its fitting curves in the region of (−0.6)−1.2 V (b). The parameters l_0, l_1, and l_2 in (a) are 196, 25, and 55 nm here, respectively. The arrows in (b) mark the positions of the charging events. The inset of (b) shows the typical AFM image of the sample surface (scan size: 1×1 μm^2 and height contrast: 8 nm).

V), s_2 (0.696 V), WL (0.821 V), and 2DEG (1.719 V). The charging voltages of the s_1 and s_2 features here are much higher than those of QDs, the C-V spectra of which can be found in Ref. 10. Alternatively, the charging voltages of the s_1 and s_2 states can be obtained by carefully fitting the C-V curve using two Gaussians plus a steplike background in the gate voltage region of (−0.6)−1.2 V.[15] The very good agreement between both procedures' result is shown in Fig. 1(b). To extract the origin of the charging features, C-V measurements of the sample are performed at different perpendicular magnetic fields, ranging from 0 to 11 T with an interval of 0.2 T. The resulting C-V spectra are summarized in Fig. 2. The positions of the charging peaks, obtained as shown in Fig. 1(b), show different energy dispersions with increasing the perpendicular magnetic-field, which is shown in Fig. 3.[2,16] The charging energy of the WL exhibits an almost linear dependence on the perpendicular magnetic field as expected for the lowest Landau level of a 2DEG in a magnetic

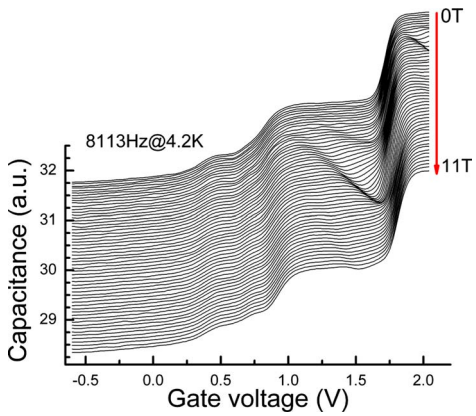

FIG. 2. (Color online) C-V spectra of the sample taken with $f=8113$ Hz at different perpendicular magnetic fields, ranging from 0 to 11 T with an interval of 0.2 T.

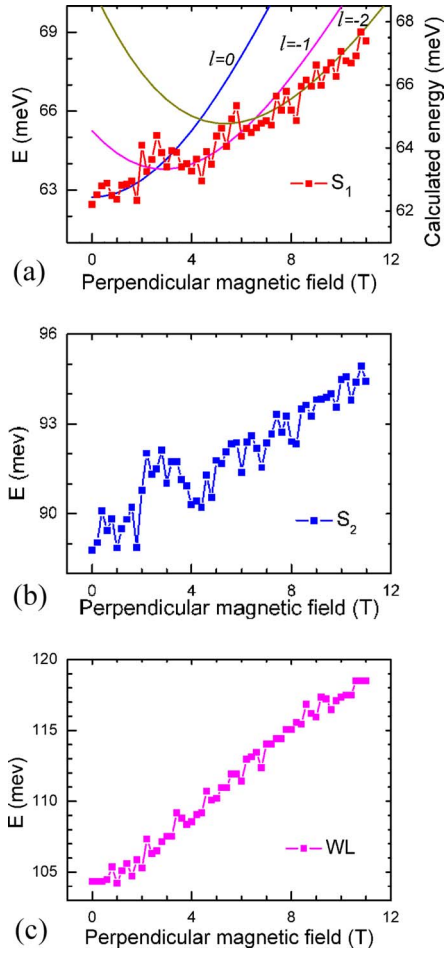

FIG. 3. (Color online) Magnetic-field dispersion of the charging energy for loading the first (a) and second (b) electron into the s-like state of the QRs, and loading electrons into the WL (c). The charging energies are obtained by using a linear lever arm approximation ($\Delta E=e\Delta V_g/\lambda$, with the lever arm $\lambda=l_0/l_1$). The solid lines ($l=0$, −1, and −2) in (a) show a fit to the experimental data.

field. However, the charging energies of the s_1 and s_2 do not increase linearly with increasing the perpendicular magnetic field. Also, they do not show the simple diamagnetic shift observed for QDs. There are two visible changes in gradient of the dispersion of both s_1 and s_2 as follows: one around 2.8 T, the other around 5.8 T. Compared with the previous theoretical and experimental data of the QRs,[2,16] the changes in gradient in the $E(B)$ in Fig. 3 can be related to a ground state transition from $l=0$ to −1 at 2.8 T, and a ground state transition from $l=-1$ to −2 at 5.8 T for the QRs, respectively. The solid lines in Fig. 3(a) show a fit to the experimental data, using a circular, parabolic wire with a electron effective mass of 0.067 m_e, a characteristic energy ($\hbar\omega_0$) of 15 meV and a radius of 20 nm as a ring model.[2,17] The approximate agreement between the radius of the rings found on the surface and the radius obtained from the fit indicates that the morphology of the volcano-shaped islands is basically preserved during the subsequent overgrowth with GaAs. And, the number of rings observed with AFM also agrees with the number of electrons in the rings obtained from the integrated area of the s_1 peak as shown in Fig. 1(b). Interestingly, the integrated area of the s_2 peak is smaller than that of s_1 peak, the reason of which might be that some of the weakly confined rings might not have a second bound state and thus cannot be occupied with two electrons. It should be noted

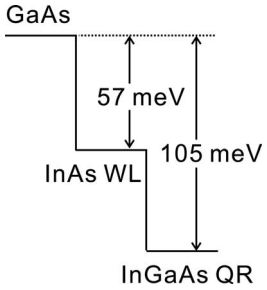

FIG. 4. Conduction band structure of the sample determined from C-V spectra and 1D numerical simulations.

that the magnetic field of the ground state transitions found here is smaller than those reported (3 and 9 T for the ground state transition from $l=0$ to -1 and the ground state transition from $l=-1$ to $l=-2$, respectively).[16] We attribute this to a somewhat larger lateral size of the present QRs. And, it is also quite surprising that the same transition fields are observed for both the one-electron and the two-electron states of the QRs. In the Aharonov–Bohm effect, the flux quantum depends on the charge of the relevant particle. So, for a two-electron state, the transition fields are expected to be reduced by approximately a factor of 2, which is not observed in our experiments. The exact reason for the observation of the same transition fields for both singly and doubly charged state is not understood at present. It should be pointed out, though, that a comparison between the far-infrared and capacitance spectroscopy suggests a similar behavior for the rings investigated in Ref. 2. Furthermore, as discussed in Ref. 5, a change in periodicity from ϕ_o/N to ϕ_o for the N-particle state can occur when the electrons are polarized or interact only weakly, or in the presence of impurities. This needs to be investigated further in future work.

As shown by the recent work on QDs,[10] C-V measurements can also be used to probe the electron energy levels of self-organized InGaAs nanostructures. As for QRs, the low density in the present sample ($\sim 1.56\times 10^{10}$ rings per cm^2, estimated from the AFM measurement) makes it reasonable to assume that the charge accumulated in the QRs is not sufficient to pin the conduction band. So, the linear lever arm approximation ($\Delta E = e\Delta V_g/\lambda$, with the lever arm $\lambda = l_0/l_1$) can be used up to the onset of the charging of the InAs WL to convert gate voltages into charging energies.[9,10,13,14] By using this linear lever arm approximation, the energetic distance from the electron ground state in the QRs to the electron ground state in InAs WL can be extracted to be $\approx$48.5 meV. Moreover, from the voltage difference between s_1 and s_2 charging peaks, the electron Coulomb blockade energy E_{ss}^C is found to be 26 meV, which is similar to the value obtained in Ref. 2. Because of its high density of states, the WL can hold a large amount of charge, which pins the conduction band and makes the lever arm approximation invalid. By using the "1D Poisson/Schrödinger" simulation[18] as described in Ref. 10, the energetic distance from the electron ground state of WL to GaAs conduction band edge in the C-V measurements here can be found to be 57 meV.[19] Combined with the energetic distance from the ground state of QRs to the ground state of WL extracted, the complete picture of the energy levels in conduction band of the QR sample can be obtained, as shown in Fig. 4. Similarly, by growing p-type doped QR samples, the valence band energy structure of the QRs can be determined as well, which provides a subject for future study.

In conclusion, a detailed C-V spectroscopy study has been performed on the self-assembled InGaAs QRs. Two well developed changes in gradient of the magnetic–field dispersion of the charging energies are observed for loading of both the first and second electron into the InGaAs QRs, which correspond to a ground state transition from $l=0$ into -1, and a ground state transition from $l=-1$ into -2, respectively. Combined with a 1D Poisson/Schrödinger simulation, the entire electron energy configuration of QRs are extracted from the C-V measurements.

This work was supported by the Bundesministerium für Bildung und Forschung (Grant Nos. 01 BM 164 and 01 BM 451) and the Australian Research Council (Grant Nos. DP0774366).

[1] D. Bimberg, M. Grundmann, and N. N. Ledentsov, *Quantum Dot Heterostructures* (Wiley, New York, 1999).
[2] A. Lorke, R. J. Luyken, A. O. Govorov, and J. P. Kotthaus, Phys. Rev. Lett. **84**, 2223 (2000).
[3] W. Lei, Y. L. Wang, Y. H. Chen, P. Jin, X. L. Ye, B. Xu, and Z. G. Wang, Appl. Phys. Lett. **90**, 103118 (2007).
[4] B. C. Lee, O. Voskoboynikov, and C. P. Lee, Physica E (Amsterdam) **24**, 87 (2004).
[5] For a review, see S. Viefers, P. Koskinen, P. Singha Deo, and M. Manninen, Physica E (Amsterdam) **21**, 1 (2004), and the references therein.
[6] N. A. J. M. Kleemans, I. M. A. Bominaar-Silkens, V. M. Fomin, V. N. Gladilin, D. Granados, A. G. Taboada, J. M. García, P. Offermans, U. Zeitler, P. C. M. Christianen, J. C. Maan, J. T. Devreese, and P. M. Koenraad, Phys. Rev. Lett. **99**, 146808 (2007).
[7] R. J. Warburton, C. Schaflein, D. Haft, F. Bickel, A. Lorke, K. Karrai, J. M. Garcia, W. Schoenfeld, and P. M. Petroff, Nature (London) **405**, 926 (2000).
[8] S. Sanguinetti, M. Abbarchi, A. Vinattieri, M. Zamfirescu, M. Gurioli, T. Mano, T. Kuroda, and N. Koguchi, Phys. Rev. B **77**, 125404 (2008).
[9] H. Drexler, D. Leonard, W. Hansen, J. P. Kotthaus, and P. M. Petroff, Phys. Rev. Lett. **73**, 2252 (1994).
[10] W. Lei, M. Offer, A. Lorke, C. Notthoff, C. Meier, O. Wibbelhoff, and A. D. Wieck, Appl. Phys. Lett. **92**, 193111 (2008).
[11] J. M. García, G. Medeiros-Ribeiro, K. Schmidt, T. Ngo, J. L. Feng, A. Lorke, J. Kotthaus, and P. M. Petroff, Appl. Phys. Lett. **71**, 2014 (1997).
[12] P. Offermans, P. M. Koenraad, J. H. Wolter, D. Granados, J. M. García, V. M. Fomin, V. N. Gladilin, and J. T. Devreese, Appl. Phys. Lett. **87**, 131902 (2005).
[13] D. Granados and J. M. García, Nanotechnology **16**, S282 (2005).
[14] C. Bock, K. H. Schmidt, U. Kunze, S. Malzer, and G. H. Döhler, Appl. Phys. Lett. **82**, 2071 (2003).
[15] Fitting model: $C(V)=C_{BK}+(A_{s1}/\sqrt{\pi/2})\times\exp\{-2[(V-V_{s1})/w_{s1}]^2\}+(A_{s2}/\sqrt{\pi/2})\times\exp\{-2[(V-V_{s2})/w_{s2}]^2\}$, where C_{BK} represents the steplike background ($C_{BK}(V)=C_0+A_0\times V+A_1/\{1+\exp[(V_1-V)/w_1]\}$, C_0, A_0, V_1, and w_1 are fitting parameters of the steplike background); A_{s1}, V_{s1}, w_{s1}, A_{s2}, V_{s2}, and w_{s2} are fitting parameters of the two Gaussian components. For more details of the fitting procedure, please see the Diploma thesis of Christian Notthoff, Universität Duisburg-Essen, Germany, 2004, unpublished, http://aglorke.uni-duisburg.de/ag_lorke/people/notthoff/diplomarbeit_chr_notthoff.pdf
[16] I. Filikhin, V. M. Suslov, and B. Vlahovic, Phys. Rev. B **73**, 205332 (2006).
[17] T. Chakraborty and P. Pietiläinen, Phys. Rev. B **50**, 8460 (1994).
[18] G. L. Snider, *Computer Program 1D Poisson/Schrödinger: A Band Diagram Calculator*, (http://www.nd.edu/~gsnider, University of Notre Dame, Indiana, America).
[19] A 1.2 nm $In_{0.38}Ga_{0.62}As$ was chosen as the InAs WL to reproduce the 0.9 V gate voltage difference between the charging of the WL and the 2DEG in the 1D Poisson/Schrödinger simulation.